VIBRATIONS OF A MICROPADDLE WITH PERIODIC AUXETIC CORE

LIGIA MUNTEANU[1], VETURIA CHIROIU[1], TUDOR SIRETEANU[1], LAZARUS TENEK[2]

Abstract. This paper discusses the vibrations of a micropaddle made from a foil with periodic auxetic core. Two major levels of complexity are discussed in order to understand the structure of this composite, and the auxetic role on the distribution of vibrations over selected frequency 'pass' and 'stop' bands. The required impedance mismatch is obtained by alternating periodically in the core regular and auxetic honeycombs. The auxeticity is interpreted in the light of Cosserat elasticity which admits degrees of freedom not present in classical elasticity.

Key words: micropaddle, auxetic honeycomb, Cosserat theory, vibration analysis.

1. INTRODUCTION

A periodic structure is a repetitive structural assembly made of a number of identical components. By integrating the material with negative Poisson's ratio (auxetic material), the stiffening geometric effect leads to increased in-plane indentation resistance, shear modulus and compressive strength, and a change in mass density [1–3]. Auxetic honeycomb's elastic and inertial properties could be selected to modify the vibration characteristics in order to fit given transmissibility specifications [4].

In Fig. 1a, a foil with a random distribution of auxetic foam is displayed. The embedded auxetic foam exhibits pores with average diameter around 20 nm. Fig. 1b displays a square honeycomb core foil. The periodicity is introduced by alternating in the core two solids with different geometry. The auxetic foam is considered because of the dependence of its mass and elastic characteristics of the cell internal angle.

The auxetic material is an attractive material which is usually used for controlling and manipulating pattern of vibration into composites. Applications, such as acoustic filters, sound insulation devices, sonic composites that impede the motion of the wave and vibrations only at selected frequency bands, may be

[1] Institute of Solid Mechanics of the Romanian Academy, Ctin Mille 15, Bucharest 010141.
[2] "Aristotle" University of Thessaloniki, Dept. of Archtectural Engineering, Thessaloniki 54124.

Rev. Roum. Sci. Tech. – Méc. Appl., Tome 55, Nº 2, P. 101–114, Bucarest, 2010

desirable in many fields [5, 6]. It has been demonstrated [7, 8] that the propagation and attenuation of vibrations in auxetic composites occurs only over selected frequency bands called ‘pass’ and ‘stop’ bands.

This work makes an analysis of the vibration pattern for a microfoil with periodic auxetic core. The required impedance mismatch is obtained by alternating periodically in the core regular and auxetic honeycombs. The auxetic material is modeled as a chiral Cosserat media. The source of chirality consists in the existence of a large number of van der Waals contacts and much fewer covalent linkages, which make possible the polymer chain to easily deform and fill any newly created free spaces. The properties of these materials are described by a modulus tensor which changes under an inversion.

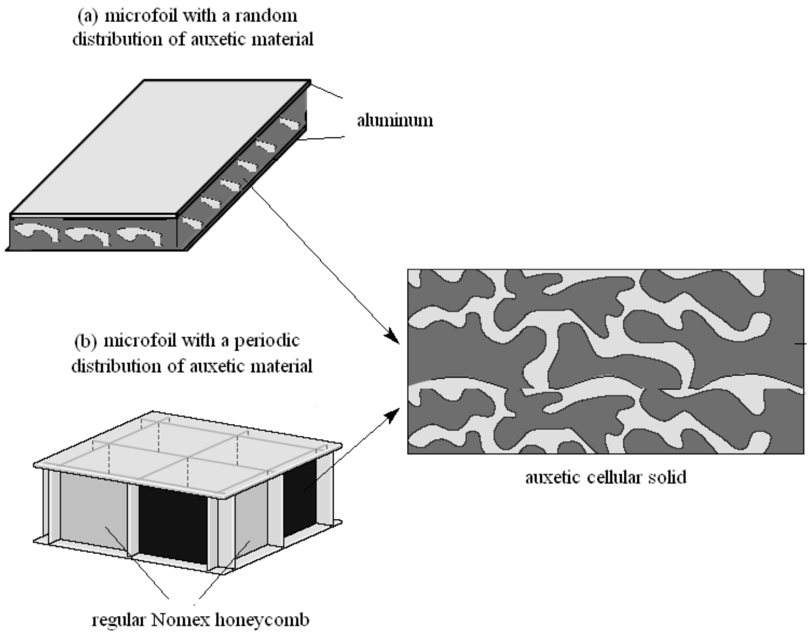

Fig. 1 – Microfoil with: a) random distribution of auxetic material; b) periodic distribution of auxetic material.

2. THE AUXETIC MATERIAL

Materials with negative Poisson’s ratio are termed by Evans *et al.* [9] as auxetic materials. The term *auxetic* is coming from the Greek word *auxetos*, meaning *that which may be increased*. Instead of getting thinner like an elongated elastic band when stretched, an auxetic material gains volume, expanding laterally. Auxetic materials and their negative Poisson’s ratios have not been well understood. Materials of this type are expected to have interesting mechanical properties, such as high energy absorption, fracture toughness, indentation resistance and enhanced shear moduli, which may be useful in some applications [10–14]. In the case of an isotropic material, the range of Poisson's ratio is from -1.0 to 0.5, based on thermodynamic considerations of strain energy in the theory of elasticity. Love [15] presented an example of a cubic single crystal pyrite as having the Poisson's ratio of -0.14, and he suggested that the effect may be caused by twinned crystals.

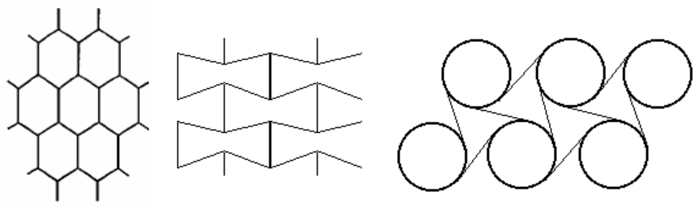

Fig. 2 – Conventional honeycomb network, re-entrant honeycomb and hexagonal structures, with negative Poisson's ratio.

The auxetic behavior is found in materials from molecular and microscopic levels up to the macroscopic level. Negative Poisson's ratios are observed in real materials with a high degree of anisotropy, such as conventional honeycomb network, re-entrant honeycomb and hexagonal structures (Fig. 2), reticulated metal foams, the skin covering a cow's teats, certain rocks and minerals, living bone tissue, etc.

3. THEORY OF COSSERAT

Generalized continuum mechanics theories admit degrees of freedom not considered in the classical theory of elasticity [16–24]. These theories have applications in modeling of materials with microstructure, such as auxetic materials. The auxetic material is not invariant to coordinates inversions and therefore can have a qualitatively different behavior in comparison with isotropic solids.

An elastic chiral material (non-centrosymmetric material) is isotropic with respect to coordinate rotations but not with respect to inversions. Chiral effects cannot be expressed within classical elasticity since, which is of the fourth rank, is unchanged under an inversion. The chirality effects in elastic materials can be described by Cosserat elasticity.

Materials may exhibit chirality on the atomic scale, as in quartz, sugar and in biological molecules. Materials may also be chiral on a larger scale, as in bones, porous materials, composites containing twisted or spiraling fibers, composites with helical or screw-shaped inclusions. The effects of chirality in elastic materials can be described by Cosserat elasticity. A chiral Cosserat material has three new elastic constants in addition to the six considered in the isotropic micropolar solid. Tensor properties of odd rank are zero if there is inversion symmetry, and can only be nonzero if there is hardness.

Consider a chiral Cosserat medium, in a Cartesian coordinates system (x,y,z). The equations of motion for the case without body forces and body couples are ([25, 26])

$$\sigma_{kl,k}-\rho\ddot{u}_l=0\,,\quad m_{rk,r}+\varepsilon_{klr}\sigma_{lr}-\rho j\ddot{\varphi}_k=0\,, \tag{1}$$

where σ_{kl} is the stress tensor, m_{kl} is the couple stress tensor, u is the displacement vector, φ_k is the microrotation vector which in Cosserat elasticity is cinematically distinct from the macrorotation vector $r_k=\frac{1}{2}\varepsilon_{klm}u_{m,l}$, and ε_{klm} is the permutation symbol. We remember that φ_k refers to the rotation of points themselves, while r_k refers to the rotation associated with movement of nearby points. In (1), ρ is the mass density and j the microinertia. The constitutive equations are

$$\sigma_{kl}=\lambda e_{rr}\delta_{kl}+(2\mu+\kappa)e_{kl}+\kappa\varepsilon_{klm}(r_m-\varphi_m)+C_1\varphi_{r,r}\delta_{kl}+C_2\varphi_{k,l}+C_3\varphi_{l,k}\,, \tag{2a}$$

$$m_{kl}=\alpha\varphi_{r,r}\delta_{kl}+\beta\varphi_{k,l}+\gamma\varphi_{l,k}+C_1e_{rr}\delta_{kl}+(C_2+C_3)e_{kl}+(C_3-C_2)\varepsilon_{klm}(r_m-\varphi_m)\,, \tag{2b}$$

where $e_{kl}=\frac{1}{2}(u_{k,l}+u_{l,k})$ is the macrostrain vector, λ and μ are the Lamé elastic constants, κ is the Cosserat rotation modulus, α,β,γ are the Cosserat rotation gradient moduli, and C_i, $i=1,2,3$ are the chiral elastic constants associated with noncentrosymmetry. For $C_i=0$ the equations of isotropic micropolar elasticity are recovered. For $\alpha=\beta=\gamma=\kappa=0$, (1) reduces to the constitutive equations of classical isotropic linear elasticity theory. From the requirement that the internal energy must be nonnegative (the material is stable), we obtain restrictions on the micropolar elastic constants $0\le 3\lambda+2\mu+\kappa$, $0\le 2\mu+\kappa$, $0\le\kappa$, $0\le 3\alpha+\beta+\gamma$, $-\gamma\le\beta\le\gamma$, $0\le\gamma$, and any positive or negative C_1,C_2,C_3.

The initial conditions are

$$u_i(x,y,z,0)=u_i^0(x,y,z)\,,\quad \varphi_i(x,y,z,0)=0\,,\quad i=1,2,3\,, \tag{3a}$$

$$m_{ij}(x,y,z,0)=0\,,\quad \sigma_{ij}(x,y,z,0)=0\,,\quad i=j\neq 3\,. \tag{3b}$$

For simplicity, without loss of generality, the particular 2D case in which all quantities depend only on x and z is considered [25, 26].

Definition 1. Let $\mathbb{F}=\{\sigma_{kl},m_{kl},u_k,\varphi_k,\ k,l=1,2,3\}$ be a set composed of the asymmetric tensors σ_{kl}, m_{kl}, e_{kl}, $k,l=1,2,3$, and the vectors u_k, φ_k. We call $\mathbb{F}$ an elastodynamic state on the bounded medium, if it satisfies equations (1)-(3).

The theory is based on the following theorem:

THEOREM 1. *The one-by-one transformation*

$$\hat{u}_1=K_{10}^2(u_1+u_2-u_3)\,,\ \hat{u}_2=K_{11}^2(u_2+u_3-u_1)\,,\ \hat{u}_3=K_{12}^2(u_3+u_1-u_2)\,, \tag{4a}$$

$$\hat{\varphi}_1=K_{10}^2(\varphi_1+\varphi_2-\varphi_3)\,,\ \hat{\varphi}_2=K_{11}^2(\varphi_2+\varphi_3-\varphi_1)\,,\ \hat{\varphi}_3=K_{12}^2(\varphi_3+\varphi_1-\varphi_2)\,, \tag{4b}$$

with

$$K_{10}^2=\frac{(C_2+C_3)^2}{4(2\mu+\kappa)(\beta+\gamma)}\,,\quad K_{11}^2=\frac{(C_2-C_3)^2}{4(2\mu+\kappa)(\gamma-\beta)}\,,$$
$$K_{12}^2=\frac{(3C_1+C_2+C_3)^2}{4(3\lambda+2\mu+\kappa)(3\alpha+\beta+\gamma)}\,, \tag{4c}$$

transforms the elastodynamic state $\mathbb{F}$ *into another elastodynamic state* $\hat{\mathbb{F}}=\{\hat{\sigma}_{kl},\hat{m}_{kl},\hat{u}_k,\hat{\varphi}_k,k,l=1,2,3\}$*, composed by the symmetric tensors* $\hat{\sigma}_{kl}$*,* $\hat{m}_{kl}$*,* $\hat{e}_{kl}$*,* $k,l=1,2,3$*, and the vectors* $\hat{u}_k$*,* $\hat{\varphi}_k$*, that satisfies (1)-(3). The state* $\hat{\mathbb{F}}$ *can be decomposited in the form*

$$\hat{\mathbb{F}}=\hat{\mathbb{F}}_1+\hat{\mathbb{F}}_2\,, \tag{5}$$

where $\hat{\mathbb{F}}_1=\{\hat{\sigma}_{11},\hat{\sigma}_{13},\hat{\sigma}_{33},\hat{m}_{22},\hat{u}_1,\hat{u}_3,\hat{\varphi}_2\}$ *and* $\hat{\mathbb{F}}_2=\{\hat{\sigma}_{22},\hat{m}_{11},\hat{m}_{13},\hat{m}_{33},\hat{u}_2,\hat{\varphi}_1,\hat{\varphi}_3\}$.

Proof. The proof is immediate. We have $\hat{e}_{kl}=\frac{1}{2}(\hat{u}_{k.l}+\hat{u}_{l,k})=\hat{e}_{lk}$, and from (2) we obtain $\hat{\sigma}_{kl}=\hat{\sigma}_{lk}$, $\hat{m}_{kl}=\hat{m}_{lk}$. The state $\hat{\mathbb{F}}$ verifies equations (1)-(3). Then, we introduce (2) into (1). After a proper combination of equations, the following equations in $\hat{u}=(\hat{u}_1,\hat{u}_2,\hat{u}_3)$ and $\hat{\varphi}=(\hat{\varphi}_1,\hat{\varphi}_2,\hat{\varphi}_3)$ are found:

$$(\lambda+2\mu+\kappa)\nabla\nabla\hat{u}-(\mu+\kappa)K_0^2\nabla\times\nabla\times\hat{u}+\kappa(1-K_0^2)\nabla\times\hat{\varphi}=\rho\ddot{\hat{u}}\,, \tag{6a}$$

$$(\alpha+\beta+\gamma)\nabla\nabla\hat{\varphi}-\gamma K_0^2\nabla\times\nabla\times\hat{\varphi}+\kappa(1-K_0^2)\nabla\times\hat{u}-2\kappa(1-K_0^2)\hat{\varphi}=\rho j\ddot{\hat{\varphi}}\,, \tag{6b}$$

with a coupling coefficient K_0 defined as

$$K_0^2=1+\frac{(C_1+C_2+C_3)^2}{(\lambda+2\mu+\kappa)(\alpha+\beta+\gamma)}\,. \tag{7}$$

We see that equations (6) are decoupled into two sets of equations in $\hat{\mathbb{F}}_1$ and $\hat{\mathbb{F}}_2$.

In the following, we will concentrate only on the set of equations corresponding to $\hat{\mathbb{F}}_1$, the other set being solved in a similar way. Let us introduce the dimensionless quantities

$$x'=\frac{\omega}{c_1}x\,,\quad z'=\frac{\omega}{c_1}z\,,\quad v_i'=\frac{\omega}{c_1}\hat{u}_i\ \ (i=1,2),\quad \phi_2'=\frac{\mu K_0^2}{\rho j\omega^{*2}}\hat{\varphi}_2\,,\quad t'=\omega t\,,$$

$$\sigma_{ij}'=\frac{1}{\mu K_0^2}\hat{\sigma}_{ij}\,,\quad m_{ij}'=\frac{c_1}{\gamma\omega K_0^2}\hat{m}_{ij}\ \ (i,j=1,3),\quad \omega^2=\frac{\kappa(1-K_0^2)}{\rho j}\,,\quad c_1^2=\frac{\lambda+2\mu+\kappa}{\rho}\,.$$

By suppressing the dashes, the equations reduce to

$$v_{1,xx}+(1-a^2)v_{3,xz}+a^2v_{1,zz}-s_4^*\phi_{2,z}=\frac{1}{s_1+s_2}\ddot{v}_1\,, \tag{8a}$$

$$v_{3,zz}+(1-a^2)v_{1,xz}+a^2v_{3,xx}+s_4^*\phi_{2,x}=\frac{1}{s_1+s_2}\ddot{v}_3\,, \tag{8b}$$

$$\phi_{2,xx}+\phi_{2,zz}-\frac{2c_1^2\kappa(1-K_0^2)}{\omega^2\gamma K_0^2}\phi_2+\frac{c_1^2\mu}{\omega^2\gamma}(v_{1,z}-v_{3,x})=\frac{1}{s_4}\ddot{\phi}_2\,, \tag{8c}$$

where

$$s_1=\frac{\lambda+\mu K_0^2}{\rho c_1^2}\,,\quad s_2=\frac{\kappa(1-K_0^2)+\mu K_0^2}{\rho c_1^2}\,,\quad s_3=\frac{\kappa j(1-K_0^2)\omega^{*2}}{\mu K_0^2c_1^2}\,,$$
$$s_4=\frac{\gamma K_0^2}{\rho j c_1^2}\,,\quad a^2=\frac{s_2}{s_1+s_2}\,,\quad s_4^*=\frac{s_3}{s_1+s_2}\,. \tag{9}$$

The initial conditions (3) become

$$v_i(x,y,0)=v_i^0\,,\ \ i=1,3\,,\qquad \phi_2(x,y,0)=0\,. \tag{10}$$

To solve the equations (8)-(10), let us consider the Laplace and Fourier transforms [27]

$$\{\overline{v}_i(x,z,p),\overline{\phi}_2(x,z,p)\} = \int_0^\infty \{v_i(x,z,t),\phi_2(x,z,t)\}\exp(-pt)\mathrm{d}t\,, \quad i=1,3\,, \tag{11}$$

$$\{\tilde{v}_i(\xi,z,p),\tilde{\phi}_2(\xi,z,p)\} = \int_0^\infty \{\overline{v}_i(x,z,p),\overline{\phi}_2(x,z,p)\}\exp(\mathrm{i}\xi x)\mathrm{d}x\,, \quad i=1,3\,. \tag{12}$$

By applying these transforms to (8), we obtain

$$\tilde{v}_1'' = \frac{1}{a^2}\left(\xi^2 + \frac{p^2}{s_1+s_2}\right)\tilde{v}_1 + \frac{\mathrm{i}\xi(1-a^2)}{a^2}\tilde{v}_3' + \frac{s_4^*}{a^2}\tilde{\phi}_2'\,, \tag{13a}$$

$$\tilde{v}_3'' = \left(a^2\xi^2 + \frac{p^2}{s_1+s_2}\right)\tilde{v}_3 + \mathrm{i}\xi s_4^*\tilde{\phi}_2 + \mathrm{i}\xi(1-a^2)\tilde{v}_1'\,, \tag{13b}$$

$$\tilde{\phi}_2'' = \frac{c_1^2\mu}{\omega^2\gamma}\tilde{v}_1' - \frac{\mathrm{i}\xi c_1^2\mu}{\omega^2\gamma}\tilde{v}_3 + \left(\xi^2 + \frac{2c_1^2\kappa(1-K_0^2)\mu}{\omega^2\gamma K_0^2} + \frac{\rho^2}{s_4}\right)\tilde{\phi}_2\,. \tag{13c}$$

An eigenvalue problem is obtained by taking the solutions of (13) of the form

$$W(\xi,z,p) = X(\xi,p)\exp(qz)\,, \tag{14}$$

where $W(\xi,z,p) = \{\tilde{v}_1,\tilde{v}_3,\tilde{\phi}_2\}$. The characteristic equation becomes

$$q^3 - \lambda_1 q^2 + \lambda_2 q + \lambda_3 = 0\,, \tag{15}$$

with

$$\lambda_1 = \left(1+\frac{1}{a^2}\right)\frac{p^2}{s_1+s_2} + 3\xi^2 + \frac{2c_1^2\kappa(1-K_0^2)}{\omega^2\gamma K_0^2} + \frac{p^2}{s_4} - \frac{2c_1^2\mu s_4^*}{\omega^2\gamma a^2}\,, \tag{16a}$$

$$\begin{aligned}\lambda_2 = &\left(\xi^2 + \frac{2c_1^2\kappa(1-K_0^2)}{\omega^2\gamma K_0^2} + \frac{p^2}{s_4}\right)\left(\frac{p^2}{s_1+s_2}\left(1+\frac{1}{a^2}\right) + 2\xi^2\right) - \\ &-\frac{c_1^2\mu s_4^*}{\omega^2\gamma a^2}\left(\frac{p^2}{s_1+s_2} + 2\xi^2\right) + \frac{1}{a^2}\left(\frac{p^2}{s_1+s_2} + \xi^2\right)\left(\frac{p^2}{s_1+s_2} + a^2\xi^2\right),\end{aligned} \tag{16b}$$

$$\lambda_3=\frac{1}{a^2}\left(\xi^2+\frac{p^2}{s_1+s_2}\right)\left(\frac{p^2}{s_1+s_2}+a^2\xi^2\right)\left(\frac{p^2}{s_4}+\xi^2+\frac{2c_1^2\kappa(1-K_0^2)}{\omega^2\gamma K_0^2}\right)-
-\frac{s_4^*}{a^2}\left(\frac{p^2}{s_1+s_2}+\xi^2\right)\xi^2\frac{c_1^2\mu}{\omega^2\gamma}. \tag{16c}$$

The roots of (15) are $q_i, i=1,2,3$, with real parts positive. The eigenvector $X(\xi,p)$ is

$$X_{i1}(\xi,p)=\begin{vmatrix}a_iq_i\\ b_i\\ -\xi\end{vmatrix},\quad X_{i2}(\xi,p)=\begin{vmatrix}a_iq_i^2\\ b_iq_i\\ -\xi q_i\end{vmatrix},\quad i=1,2,3, \tag{17a}$$

$$a_i\Delta_i=\xi(a^2-1)\left(\left(\xi^2+\frac{2c_1^2\kappa(1-K_0^2)}{\omega^2\gamma K_0^2}+\frac{p^2}{s_4}\right)-q_i^2\right)-\frac{c_1^2\mu s_4^*\xi}{\omega^2\gamma}, \tag{17b}$$

$$\mathrm{i}b_i\Delta_i=\left(\xi^2+\frac{p^2}{s_1+s_2}\right)\left(\xi^2+\frac{2c_1^2\kappa(1-K_0^2)}{\omega^2\gamma K_0^2}+\frac{p^2}{s_4}\right)+
+a^2q_i^2\left(q_i^2-\xi^2+\frac{2c_1^2\kappa(1-K_0^2)}{\omega^2\gamma K_0^2}+\frac{p^2}{s_4}\right)-\left(\xi^2+\frac{p^2}{s_1+s_2}\right)q_i^2+\frac{c_1^2\mu s_4^*q_i^2)}{\omega^2\gamma}, \tag{17c}$$

$$\Delta_i=\frac{c_1^2\mu}{\omega^2\gamma}\left(q_i^2-\left(\xi^2+\frac{p^2}{s_1+s_2}\right)\right),\quad i=1,2,3. \tag{17d}$$

So, the solution (14) becomes

$$W(\xi,z,p)=\sum_{i=1}^{3}B_iX_i(\xi,p)\exp(q_i(\xi,p)z), \tag{18}$$

where B_i, $i=1,2,3$, are arbitrary constants. Using (18), the transformed displacement, microrotation and stresses are given by

$$\tilde{v}_1(\xi,z,p)=a_1(\xi,p)q_1(\xi,p)B_1\exp(q_1(\xi,p)z)+
+a_2(\xi,p)q_2(\xi,p)B_2\exp(q_2(\xi,p)z)+a_3(\xi,p)q_3(\xi,p)B_3\exp(q_3(\xi,p)z)\}, \tag{19}$$

$$\tilde{v}_3(\xi,z,p)=b_1(\xi,p)B_1\exp(q_1(\xi,p)z)+b_2(\xi,p)B_2\exp(q_2(\xi,p)z)+
+b_3(\xi,p)B_3\exp(q_3(\xi,p)z)\}, \tag{20}$$

$$\tilde{\phi}_2(\xi, z, p) = -\xi\{B_1 \exp(q_1(\xi, p)z) + B_2 \exp(q_2(\xi, p)z) + B_3 \exp(q_3(\xi, p)z)\}\,. \quad (21)$$

To obtain the unknowns B_i, $i = 1,2,3$, we apply the Laplace and Fourier transforms on initial conditions (10)

$$\tilde{v}_i(\xi, z, 0) = \tilde{v}_i^0\,,\ \ i = 1,3\,, \qquad \phi_2(x, y, 0) = 0\,. \quad (22)$$

The transformed quantities are functions of z and of the parameters of Laplace and Fourier transforms p and ξ, and are of the form $f(\xi, z, p)$. To obtain the function $f(x, z, t)$, first we invert the Fourier transform by using

$$\overline{f}(x, z, p) = \frac{1}{2\pi}\int_{-\infty}^{\infty} \exp(-\mathrm{i}\xi x)\tilde{f}(\xi, z, p)\mathrm{d}\xi = \frac{1}{\pi}\int_{0}^{\infty}\{\cos(\xi x) f_e - \mathrm{i}\sin(\xi x) f_0\}\mathrm{d}\xi\,, \quad (23)$$

where f_e and f_0 are even and odd parts of the function $\tilde{f}(\xi, z, p)$ respectively. Expression (23) gives the Laplace $\overline{f}(x, z, p)$ of the function $f(x, z, t)$. For the fixed values of ξ, x and z, the $\overline{f}(x, z, p)$ in (23) can be considered as the Laplace transform $\overline{g}(p)$ of some function $g(t)$. The function $g(t)$ can be obtained by using

$$g(t) = \frac{1}{2\pi\mathrm{i}}\int_{C-\mathrm{i}\infty}^{C+\mathrm{i}\infty} \exp(pt)\overline{g}(p)\mathrm{d}p\,, \quad (24)$$

where C^0 is an arbitrary real number greater than all the real parts of the singularities $\overline{g}(p)$. For $p = C^0 + \mathrm{i}y$ we have

$$g(t) = \frac{\exp(C^0 t)}{2\pi}\int_{-\infty}^{\infty} \exp(\mathrm{i}ty)\overline{g}(C^0 + \mathrm{i}y)\mathrm{d}y\,. \quad (25)$$

4. RESULTS

This paper discusses the vibrations of a microfoil with a periodic distribution of the auxetic material (Fig. 1b). This foil pays the role of a micropaddle resonator. The geometry of the paddle is displayed in Fig. 3. The regular honeycomb core is made of Nomex (Young's modulus E = 1.55 GPa, density ρ = 37 kg/m^2 and Poisson's ratio ν = 0.25). The auxetic core has a negative Poisson's ratio $\nu = -0.35$.

The following dimensions are taken: $l = 2.5\,\mu\text{m}$, $a = 2\,\mu\text{m}$, $b = 3.5\,\mu\text{m}$, $d = 200\,\mu\text{m}$, $c = 175\,\mu\text{m}$, and an asymmetry of about $d_{asim} = 40\,\mu\text{m}$. The force per unit on the paddle was assumed to be $f = 200\ \text{N}{\cdot}\text{m}^{-2}$.

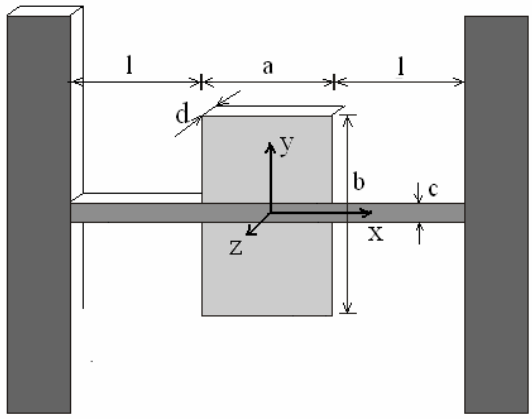

Fig. 3 – The geometry of the paddle resonator (microfoil).

The motion of the paddle is very complex [28, 29]. It combines the translational, bending and torsional motions. These types of motions are treated together in a unitary manner. The first four natural frequency of the paddle (translational-bending-torsional modes) are given by 15.81 MHz, 45.33 MHz, 71.77 MHz and 129.14 MHz. Fig. 4 displays the first two coupled modes of the paddle.

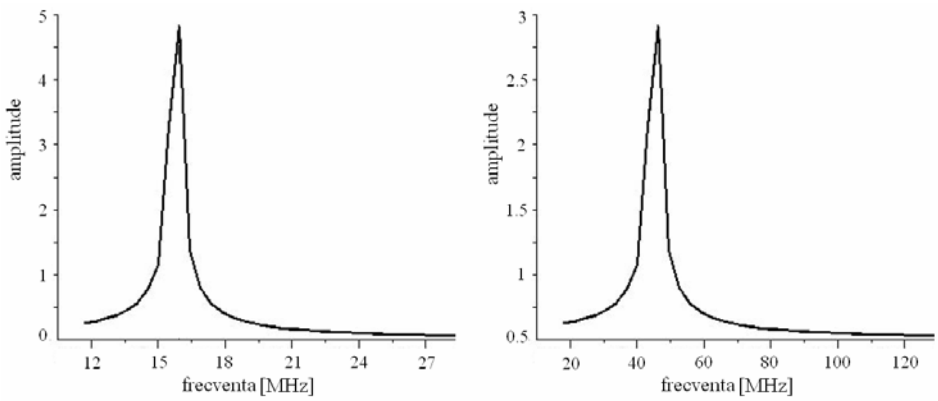

Fig. 4 – First and second coupled modes.

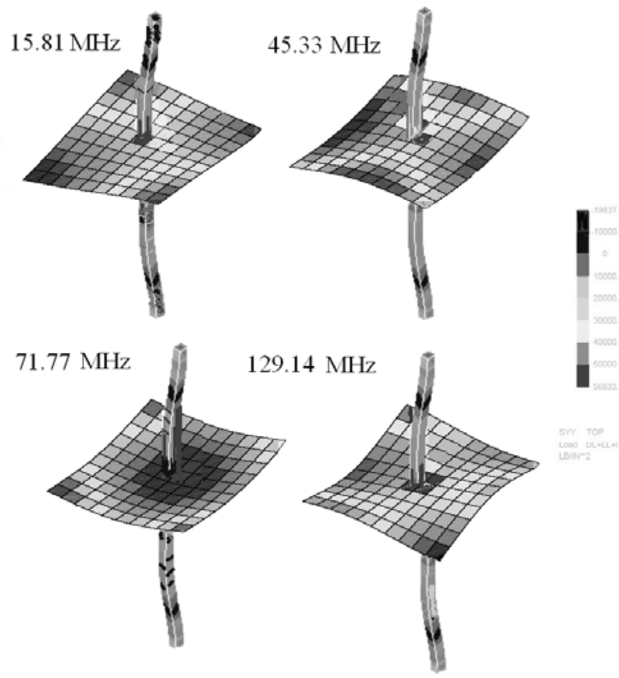

Fig. 5 – Stress distribution for the first four coupled modes.

The stress distribution in the paddle is represented in Fig. 5, for the first four coupled modes. Honeycomb core materials of different geometry placed periodically along the structure introduce the impedance mismatch necessary to obstruct the vibrations over specific frequency bands (stop bands). The impedance mismatch can be easily tuned through the choice of the appropriate material properties and geometry of the materials composing the core. The impedance mismatch can be easily tuned through the choice of the appropriate material properties and geometry of the materials composing the core. The vibration pattern is displayed in Fig. 6.

Fig. 6 shows that the paddle exhibits full band-gaps in the range (12.8–15.3 MHz), where the vibration is not allowed to propagate due to complete reflections. The band-gaps or the well-known Bragg reflections occur at different frequencies inverse proportional to the central distance between two honeycomb cells (the lattice constant). If the band-gaps are not wide enough, their frequency ranges do not overlap. These band-gaps can overlap due to reflections on the cells, as well as due to vibration propagation inside the cells. Then, the vibration is reflected completely from this periodic array of acoustic scatterers in the frequency range where all the band-gaps for the different periodical directions overlap.

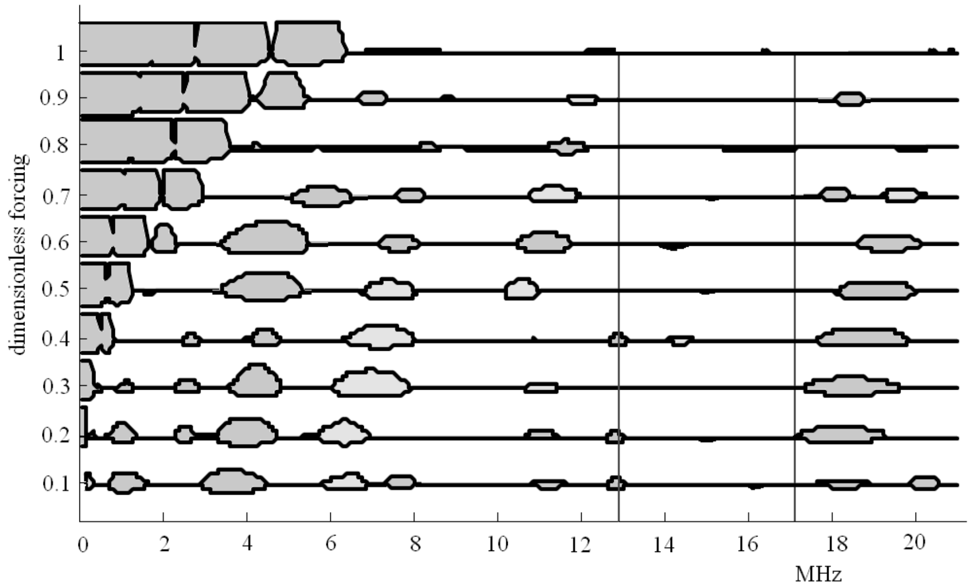

Fig. 6 – The vibration pattern.

This is the fundamental mechanism for the formation of a full band-gap which is required for photonic and sonic crystals [5]. The complete reflection on the boundaries of scatterers (cells) is due to the full band-gap property itself, and it occurs independent of the incident angle [5, 31]. The transmission of vibrations over specified frequency bands can be significantly for the active control devices without compromising the size and the weight of the structure [32].

5. CONCLUSIONS

The mechanical analysis across two levels of complexity enables the understanding of the auxetic composites properties and behavior. The major levels of complexity are structural and respectively, the computing complexity. The auxetic material is modeled with Cosserat elasticity which admits degrees of freedom not present in classical elasticity, *i.e.*, the rotation of points in the material, and a couple per unit area or the couple stress.

The description of a particular auxetic system's behavior provides a framework of the interaction between these two adjoining levels of complexity. This interaction is exemplified by considering the vibrations of a composite foil with periodic auxetic core, which pays the role of a micropaddle resonator. The auxetic role on the attenuation of vibrations over selected frequency 'pass' and 'stop' bands is discussed. The required impedance mismatch is obtained by alternating periodically in the core regular and auxetic honeycombs.

The results explain why the transmission of vibrations over specified frequency bands can be significantly reduced without additional passive or active control devices and without compromising the size and the weight of the structure.

The core geometry can be easily optimized in order to obtain attenuation over desired frequency bands. The characteristic behavior of auxetic composites in particular provides great flexibility for proper tuning of the stop bands.

ACKNOWLEDGEMENTS. The authors gratefully acknowledge the financial support of the National Authority for Scientific Research (ANCS, UEFISCSU), through PN-II research project 106/2007, code ID_247/2007.

Received on June 8, 2010

REFERENCES

1. DONESCU, Şt., CHIROIU, V., MUNTEANU, L., *On the Young's modulus of an auxetic composite structure*, Mechanics Research Communications, **36**, *3*, pp. 294-301, 2009.
2. CHIROIU, V., MUNTEANU, L., *On the behavior of beams with external damping patches*, International Journal of Nonlinear Mechanics, 2010.
3. MUNTEANU, L., CHIROIU, V., DUMITRIU, D., BALDOVIN, D., CHIROIU, C., *On the eigenfrequency optimization of Euler-Bernoulli beams with nonlocal damping patches*, Rev. Rom. Sci. Techn. – Méc. Appl., **54**, *1*, pp. 53-66, 2009.
4. MAZZARELLA, L., RUZZENE, M., TSOPELAS, P, *Spectral finite element modelling of wave propagation in sandwich plate-rows with periodic honeycomb core*, 15th ASCE Eng. Mechanics Conf., Columbia University, New York, June 2-5, 2002.
5. MUNTEANU, L., CHIROIU, V., *On the dynamics of locally resonant sonic composites*, European Journal of Mechanics – A/Solids, 2010.
6. DONESCU, Şt., MUNTEANU, L., DELSANTO, P.P., MOŞNEGUŢU, V., *On the advanced auxetic composites*, (Chap. 4), in: *Research Trends in Mechanics* – Vol. 3 (eds. D. Popa, V. Chiroiu, L. Munteanu), Romanian Academy Publishing House, Bucharest, pp. 78-93, 2009.
7. CHIROIU, V., MUNTEANU, L., DUMITRIU, D., BELDIMAN, M., SECARĂ, C., *On the architecture of a new cellular elastic material*, Proc. of the Romanian Academy, Series A: Mathematics, Physics, Technical Sciences, Information Science, **9**, *2*, pp. 105-116, 2008.
8. MEAD, D.J., *Wave propagation in continuous periodic structures: Research contributions from Southampton 1964-1995*, Journal of Sound and Vibration, **190**, *3*, pp. 495-524, 1996.
9. EVANS, K.E., NKANSAH, M.A., HUTCHINSON, I.J., ROGERS, S.C., *Molecular network design*, Nature, **353**, pp. 124-125, 1991.
10. LAKES, R.S., *Experimental Microelasticity of Two Porous Solids*, International Journal of Solids and Structures, **22**, *1*, pp. 55-63, 1986.
11. LAKES, R.S., *Foam structures with a negative Poisson's ratio*, Science, **235**, pp. 1038-1040, 1987.
12. LAKES, R.S., *Experimental micro mechanics methods for conventional and negative Poisson's ratio cellular solids as Cosserat continua*, J. Engineering Materials and Technology, **113**, *1*, pp. 148-155, 1991.
13. OVERAKER, D.W., CUITIÑO, A.M., LANGRANA, N.A., *Effects of morphology and orientation on the behavior of two-dimensional hexagonal foams and application in a re-entrant foam anchor model*, Mechanics of Materials, **29**, *1*, pp. 43-52, 1998.

14. WANG, Y.-C., LAKES, R.S., *Analytical parametric analysis of the contact problem of human buttocks and negative Poisson's ratio foam cushions*, International Journal of Solids and Structures, **39**, *18*, pp. 4825-4838, 2002.
15. LOVE A.E.H., *A treatise on the mathematical theory of elasticity*, 4th ed., Dover, New York, 1926.
16. COSSERAT, E., COSSERAT, F., *Théorie des Corps Déformables*, Hermann et Fils, Paris, 1909.
17. MINDLIN, R.D., *Microstructure in linear elasticity*, Arch. Rat. Mech. Anal., **16**, pp. 51-78, 1964.
18. MINDLIN, R.D., *Stress functions for a Cosserat continuum*, International Journal of Solids and Structures, **1**, *3*, pp. 265-271, 1965.
19. ERINGEN, A.C., *Linear Theory of Micropolar Elasticity*, J. Math. Mech., **15**, pp. 909-924, 1966.
20. ERINGEN, A.C., *Theory of micropolar elasticity*, in *Fracture* – Vol. 2, ed. R. Liebowitz, pp. 621-729, Academic Press, New York, 1968.
21. ERINGEN, A.C., *Theory of micropolar fluids*, J. Math. Mech., **16**, *1*, pp. 1-18, 1966.
22. MUNTEANU, L., CHIROIU, V., DUMITRIU, D., BELDIMAN, M., *On the characterization of auxetic composites*, Proc. of the Romanian Academy, Series A: Mathematics, Physics, Technical Sciences, Information Science, **9**, *1*, pp. 33-40, 2008.
23. TEODORESCU, P.P., CHIROIU, V., MUNTEANU, L., DONESCU, Şt., *On the behavior of advanced auxetic plate*, CESES: Computer and Experimental Simulations in Engineering and Science, *3*, pp. 106-116, 2008.
24. TENEK, L., AIFANTIS, E., *An atomistic model for localized deformation*, Journal of Mechanical Behavior of Materials*,* **18**, *1*, pp. 33-42, 2007.
25. TEODORESCU, P.P., MUNTEANU, L., CHIROIU, V., *On the wave propagation in chiral media*, in *New Trends in Continuum Mechanics*, in: *Theta Series in Advanced Mathematics* (ed. M. Mihailescu-Suliciu), Edit. Thetha Foundation, Bucharest, pp. 303-310, 2005.
26. TEODORESCU, P.P., BADEA, T., MUNTEANU, L., ONIŞORU, J., *On the wave propagation in composite materials with a negative stiffness phase*, in *New Trends in Continuum Mechanics*, in: *Theta Series in Advanced Mathematics* (ed. M. Mihailescu-Suliciu), Edit. Thetha Foundation, Bucharest, pp. 295-302, 2005.
27. POULARIKAS, A.D. (ed.), *The transforms and applications handbook* (2nd edition), Boca Raton, CRC Press, IEEE Press, 2000.
28. CHIROIU, V., MUNTEANU, L., PĂUN, V., *On the paddle resonator*, in *Nanostructuring and Nanocharacterization* – Series in Micro and Nanoengineering (eds. M. Zaharescu, M. Ciurea, D. Dascălu), Romanian Academy Publishing House, Bucharest, pp. 83-97, 2010.
29. TENEK, L., *Buckling Oscillations of a Cantilever Beam*, CESES: Computer and Experimental Simulations in Engineering and Science, *1*, pp. 34-38, 2008.
30. TENEK, L., BASKES, M., AIFANTIS, E., *An atomistic approach to the transverse shearing of single aluminum and aluminum-nickel bimaterial systems*, Journal of Mechanical Behavior of Materials, **14**, *1*, 2003.
31. MIYASHITA, T., *Full band gaps of sonic crystals made of acrylic cylinders in air – Numerical and experimental investigations*, Jpn. J. Appl. Phys., **41**, pp. 3170-3175, 2002.
32. STAMMERS, C.W., SIRETEANU, T., *Control of building seismic response by means of three semi-active friction dampers*, Journal of Sound and Vibration, **237**, *5*, pp. 745-759, 2000.